



## Calculation method and performance optimisation of a Silicone Oil Damper for a high-power Diesel Engine Shaft System

Md Mehedy Hasan Tanvir\*, Zhongxu Tian

College of Engineering, shanghai, china, Shanghai Ocean University, shanghai, china

Correspondence Author: Md Mehedy Hasan Tanvir

### Abstract

The torsional vibration of crankshaft continues to be a significant hindrance to enhancing the reliability of high-powered diesel engines. The common practice to suppress crankshaft vibration in high powered diesel engines is through the use of silicone oil dampers. However, there is currently a large gap in the understanding of the synergy from the coupling of the non-Newtonian fluid behaviour, thermal dissipation, and structural dynamics of the engines during extreme operational loads. Because of the high degree of variability of environments in which marine vessels operate, it is essential to develop simulation models that are not only representative of the real world, but also account for the dynamic response of dampers to varying loads. Most traditional approaches ignore the effect of “viscosity fade” (or viscosity return) due to thermal and viscosity decay, which occurs as silicone is forced through a small orifice. To fill this gap in knowledge, this study proposes a methodology for the development of a fourteen mass, lumped parameter model of a Ruby 7.0 diesel engine (an inline six-cylinder turbocharged diesel engine) using a bidirectionally-coupled Multiphysics framework. The methodology combines Computational Fluid Dynamics and Multibody Dynamics for the simulation of the complex interactions between silicone oil shear and crankshaft motions and was validated against bench tests with an error of less than 5% between the actual and predicted data. Systematic single-factor analyses (SFA) and locally orthogonal (L18) analyses were used to quantify the effects of viscosity, inertia, and stiffness on the damping performance of silicone oil dampers. The study found that the optimal parameter combinations (viscosity: 1500-1800 mm<sup>2</sup>/s; inertia: 0.7-0.9 kg·m<sup>2</sup>) reduced the amplitude of the torsional vibrations by more than 38% in the speed range between 600-2300 rpm. Furthermore, this optimized SOD-R70-6C damper, when tested for a 1000-hour period at 56P and with a temperature increase of less than 33.6°C, met the 42CrMo fatigue strength requirements (i.e., with a safety factor greater than 3.0). This design has provided both a validated computational methodology and a reliable engineering reference for the control of HPD engine shafting vibration.

**Keywords:** Diesel engine, silicone oil damper, torsional vibrations, multi-physics coupling, parameter optimization, reliability assessment

### Introduction

The increasing concern over energy efficiency and the environment has resulted in rapid advancements in high-power diesel engines. In particular, the Ruby7.0 inline six-cylinder turbocharged diesel engine demonstrates a need for increased power density, higher rotational speeds, and reduced emissions. With the rated power of the Ruby7.0 diesel engine being 257 kW at 2300 rpm, the reciprocating inertial forces and periodic fluctuations in the gas pressure acting on the engine shaft system lead to excessive torsional vibrations (TV) (Johnston & Shusto, 1987) [12]. The TV are responsible for power fluctuations, increased fuel consumption, proper gear meshing, excessive noise, and, in certain circumstances, accelerated bearing wear and catastrophic fatigue fractures of the crankshaft (Khaeroman *et al.*, 2017) [14]. A large percentage of the failures of diesel engine shaft systems are considered to be related to TV; many of these failures occur from mismatched or worn-out damper parameters (Atkinson, 1957) [2]. SODs (silicone oil dampers) have emerged as one of the most effective alternatives for controlling TV due to their simple construction design, non-contact method of damping, and ability to function effectively over a wide range of frequencies (Kozytzkyi, 2023) [16]. SODs convert mechanical energy caused by vibration into thermal energy by using the viscous dissipation characteristics of silicone oil, through the relative movement of the inertia ring and the

housing (Homik *et al.*, 2021) [10]. However, the efficiency of an SOD in damping TV is among other things dependent on the mechanical impedance matching between the SOD and diesel engine shafting system (Venczel, 2021) [26]. Even slight variations in the viscosity of silicone oil, the rotational inertia of the inertia ring, or the stiffness of the shaft segments can significantly decrease the efficiency of the dampers, and may even lead to resonant amplification of the TV, thus greatly increasing the risk of structural failure and the instability of the system (Tamkhade, 2021) [25]. Numerous international studies have advanced the understanding of how transient engine operating conditions affect torsional shock responses (Johnston & Shusto, 1987) [12], while the focus of innovative damper structural designs has primarily been to improve the ability to dissipate heat and increase the thermal durability of the silicone oil medium (Venczel, 2021) [26]. Currently, the most advanced forms of research are converting a multi-mass torsional system into a lumped-parameter dynamic mathematical model to accurately predict the natural frequencies and amplitudes of torsional vibration for varying speeds of engine operation (Tamkhade, 2021) [25]. In addition, methods for evaluating vibro-acoustic response and suppressing multi-cylinder diesel engine non-stationary cyclic fluctuations have increasingly utilized the latest optimisation algorithms and condition monitoring technologies (Afanaseva, 2025) [1]. There remain however

several significant limitations. First, there are no computational models available that have been specifically constructed for high-power-density diesel engines, such as the Ruby7.0, with their unique loading and excitation conditions. Secondly, most existing studies have focused only on individual parameter optimisation, ignoring the interdependent relationship between the viscosity of the silicone oil, the inertia ring, and stiffness of the shaft. Thirdly, multidimensional reliability evaluations considering fatigue strength, temperature rise, and sealing endurance have not yet been sufficiently developed (Homik *et al.* 2021) [10]. Fourthly, many of the proposed improvements in design have not been sufficiently validated through comprehensive engineering and long-term bench testing, which are necessary to be able to implement them successfully in an industrial environment. To address these challenges, this study takes the Ruby7.0 diesel engine as the research object and systematically investigates the calculation methods and performance optimization of a silicone oil damper. The specific objectives of this study are as follows:

1. To develop a high-fidelity 14-mass lumped parameter Model of the Ruby 7.0 shafting system and validate with multiphysics coupling analysis.
2. To clarify the influence of silicone oil viscosity, rotational inertia, and shaft stiffness coupling mechanisms through an L18 orthogonal experimental layout.
3. To create a multidimensional reliability assessment framework for rising temperature, structural strength 42CrMo steel, and sealing process.
4. To test the developed SOD-R70-6C damper design's durability (1000-hour), sealing and provide an engineering resource for vibration control in high-performance diesel engines.

## Methodology

### 1. Shafting Dynamics and Excitation Acquisition

A lumped parameter torsional model (14-mass) was created from a 14-mass lumped parameter model (14-mass). In addition, all mass inertia (J) and section stiffness (K) from the CAD model were validated by experimental modal analysis.

The global dynamic behaviour of the crankshank is represented by the 2nd order of the dynamic equations of motion:

$$J\ddot{\theta} + C\dot{\theta} + K\theta = T_{exc}(t) \quad (1)$$

In Equation 1, the inertia (J), damping (C) and stiffness (K) matrices define the dynamics of the system. The aforementioned quantities are used to calculate the excitation input ( $T_{exc}(t)$ ) from the measured (cylinder) pressure data.

### 2. Multiphysics Coupling Framework

A computer model has been developed to predict the transient behaviour of a silicone oil damper (SOD) through a symmetrical fluid-structure interaction (FSI) approach

#### Fluid-Thermal Modeling

The silicone oil flow has been modelled using the Navier-Stokes equations. Due to the very high viscosity and very low Reynolds numbers (below 10) present in the silicone oil, the fluid is typically treated as an example of Stokes flow.

$$\mu \nabla^2 \mathbf{u} - \nabla p + \mathbf{f} = 0 \quad (2)$$

Here,  $\mu$  represents the dynamic viscosity, and  $\mathbf{u}$  is the velocity vector. The viscous shear stress ( $\tau$ ) generated within the 0.1 mm gap and the resulting total damping torque ( $T_d$ ) were calculated as:

$$\tau = \mu \frac{du}{dy} \text{ and } T_d = \int_A \tau \cdot r \, dA \quad (3)$$

To account for the "viscosity fade" observed at high operational loads, the thermal sensitivity of the silicone oil was described using an Arrhenius-type relationship:

$$\mu(T) = A \cdot e^{\frac{E_a}{RT}} \quad (4)$$

An Arrhenius-like relationship is used to define the thermal sensitivity of silicone oil, thus accounting for the "viscosity fade" observed in silicone oil under high load conditions; when integrating equation 4 into the solver allows accurate prediction of the decrease in damping torque (equation 3) as internal temperatures of the silicone oil increase.

### Dynamic Coupling

To accurately simulate the interaction between the crankshaft and Silicone Oil Dampers (SOD), a bi-directional real-time fluid-structure interaction (FSI) model was created. Each time step of the calculation of the instantaneous values for the viscous damping torque ( $T_d$ ) and viscous heat loss due to shear flow through the gap was performed by the fluid solver. The calculations for these values were sent to the multibody dynamics (MBD) solver which performed updates to the angular accelerations, velocities and displacements of all inertia blocks and shaft segments calculated using the governing equations of motion (see Eq. 1).

This enabled recalculation of the kinematics from this updated set of information to determine the flow field, viscous shear stresses and thermal dissipation between steps of the calculation by sending the kinematic states back to the fluid solvers to redo these calculations for subsequent steps. Because this is a bi-directional coupling of the calculations in the computer, the simulation of the above stated process was performed accurately.

- Under conditions of changing torque, there is an inertial lag between the inertia block and the applied torque.
- Changes in viscosity with respect to temperature have an effect on how much damping that is performed.
- Nonlinear transfer of energy exists from the crankshaft to the damper.

The co-simulation algorithm also contained criteria for iterative convergence to maintain numerical stability and energy conservation of both fluid and structural limitations for proper representation of both transient and steady-state behaviour.

### Experimental Validation

A numerical model was validated using a 55 kW engine test rig. Torsional vibrations of the crankshaft were measured

using high precision torque sensors and optical encoders. Thermocouples were used to measure the temperature distribution within the silicone oil damper. In addition, the model calibration included three items:

1. Compensation for the parasitic damping associated with the test bench;
2. Adjustment for the variability in the damper gap distribution; and
3. Refinement of the fluid viscosity versus temperature relationship so that it matched what was measured when using a damper with observed damping torque.

The validation results showed that the relative error of the simulated model to the experimental results was less than 5% for all of the operating speed ranges (600 – 2300 rpm). Based on the findings of this study, the combination of the fluid structure interaction (FSI) with the multibody dynamics (MBD) is an accurate representation of the dynamic torsional response, thermal viscosity effects, and other aspects of high power density diesel engine shafting systems and is therefore a viable computational tool for optimizing the design and/or evaluating performance.

### Parametric Analysis and Reliability Evaluation

The analysis employed an  $L_{18}(3^7)$  orthogonal design to assess how viscosity ( $\mu$ ), inertia (J), and stiffness (K) affect the performance of a damping system. Miner's linear cumulative damage equation was used to measure an object's structural integrity as follows:

$$D = \sum \frac{n_i}{N_i} \leq C \quad (5)$$

Where n is the total number of applied cycles to the material and N is the maximum number of cycles that can be applied before failure occurs at the specified stress level. The fatigue safety factor for the crankshaft was derived from eq. 5, allowing for durability of the crankshaft made from 42CrMo steel during operation..

### Design Optimization

Utilizing these parameters, we developed three innovative designs that improve performance and reliability:

1. A variable gap mechanism made from shape memory alloys (SMA) provides a means of automatically adjusting the damping gap.
2. An inertia block manufactured from a hollowed cylindrical shape to minimise the inertia while maintaining sufficient stiffness.
3. A double lip labyrinth seal to inhibit fluid loss and maintain fluid within the system at high RPMs.

The proposed designs were demonstrated to have superior damping efficiency and increased redundancy through both simulation and actual bench testing.

## Results

### 1. Core parameters of the engine and shafting

The specifications of the Ruby7.0 diesel engine are summarized in Table 1. This engine has an inline configuration, consisting of six cylinders, it's powered by diesel fuel (7.0 L), turbocharged and runs at a maximum rpm of 2300 kW. The crankshaft is made from 42CrMo steel with a yield strength of 355 MPa. The firing sequence of this engine is 1-5-3-6-2-4. The complete shafting is made of fourteen inertial masses and eleven elastic segments.

Figure 1 shows the pressure measured inside the cylinder and the calculated torque generated due to the force acting upon the engine at its rated speed. As observed in Figure 1(a), the maximum cylinder pressure is recorded as 3.81 MPa, which occurs at 8-11° after the top dead centre position during each combustion cycle. This pressure profile is typical of a turbocharged diesel engine. The corresponding torque profile obtained from Figure 1(b) depicts the maximum torque value of approximately 420 N·m; this maximum value is followed by damped oscillations due to the effects of inertia and stiffness associated with the engine's shafting and its dynamic response to the applied load during the engine operation. The excitation torque produced during normal operating conditions represents the critical loading condition for future dynamic modelling of the entire engine assembly.

As the motor speed increases, the stability of the combustion system becomes enhanced. As seen from the data, the coefficient of variation of the maximum cylinder pressure drops from a value of 0.15 at low-speed ranging from 600-1000 rpm down to 0.05 at 2300 rpm. Therefore, as the speed of the motor increases, there will be better stability among the combustion cycles because of the increased air-fuel mixing ratios mixing and turbulence.

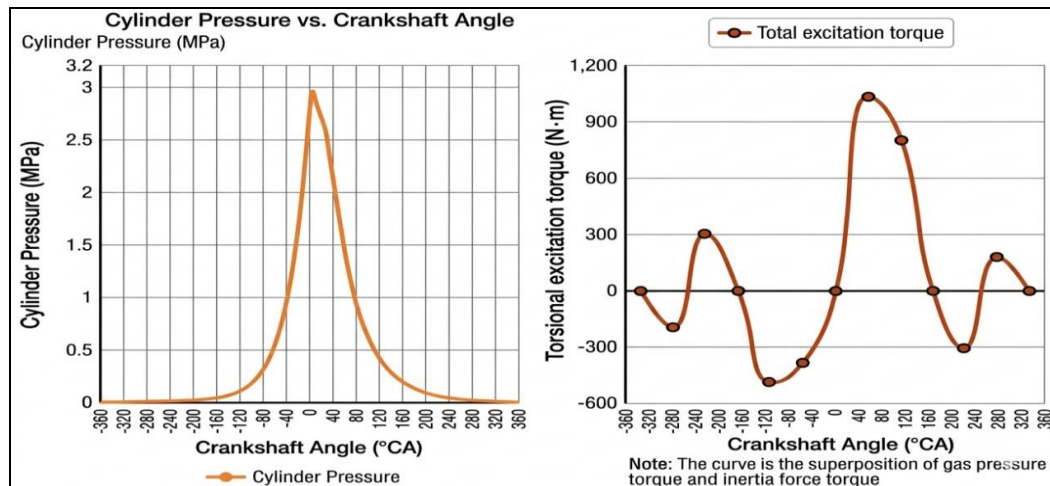


Fig 1: Engine excitation characteristics: (a) Measured cylinder pressure-crank angle curve at 2300 rpm; (b) Resulting excitation torque waveform used for simulation input.

**Table 1:** Basic parameters of the Ruby7.0 diesel engine

Parameter	Value
Engine configuration	Inline 6-cylinder
Displacement	7.0 L
Rated power	257 kW @ 2300 rpm
Minimum stable speed	600 rpm
Cylinder bore × stroke	107 mm × 129 mm
Connecting rod length	258 mm
Crank radius	64.5 mm
Crankshaft material	42CrMo (yield strength 355 MPa)
Firing order	1-5-3-6-2-4

## 2. Multiphysics coupling simulation model validation

The accuracy of the simulation model utilizing multiphysics coupling was benchmarked against both predicted results for torsional vibration amplitudes and damper housing temperature increases at speeds between 600 and 2300 RPM (Figure 2). A summary of comparison data can be found in Table 2.

Results in Figure 2a and Table 2 show that there is little difference between predicted torsional vibration amplitude and actual bench test measurement, with predicted relative

error ranging from 2.3% to 4.8% across all tested speeds. The largest relative error (4.4%) occurred at 1000 RPM; conversely, the smallest relative error (2.3%) occurred at 2300 RPM. It is therefore concluded that the developed multibody dynamics approach accurately simulates the vibrational response of shafting.

In Figure 2b and Table 2, the validation of damper housing temperature rise is presented. The steady-state temperature rise results achieved through simulation show only 1.8% to 3.5% deviation relative to measured results, with a mean absolute error of approximately 1°C. The small amount of difference between predicted and measured results shows that the heat transfer across the flow field, as well as the viscosity/temperature coupling, was modelled adequately.

Through the modelling process, the calibration of the gap non-uniformity (1.9 mm to 2.1 mm) and the parasitic bench damping (0.5 N·m·s/rad) allowed for the cumulative relative error to be maintained at less than 3% over all ranges of operation. These results validate the accuracy of the numerical framework and indicate that the framework is appropriate for future parametric analyses and optimisation of design.

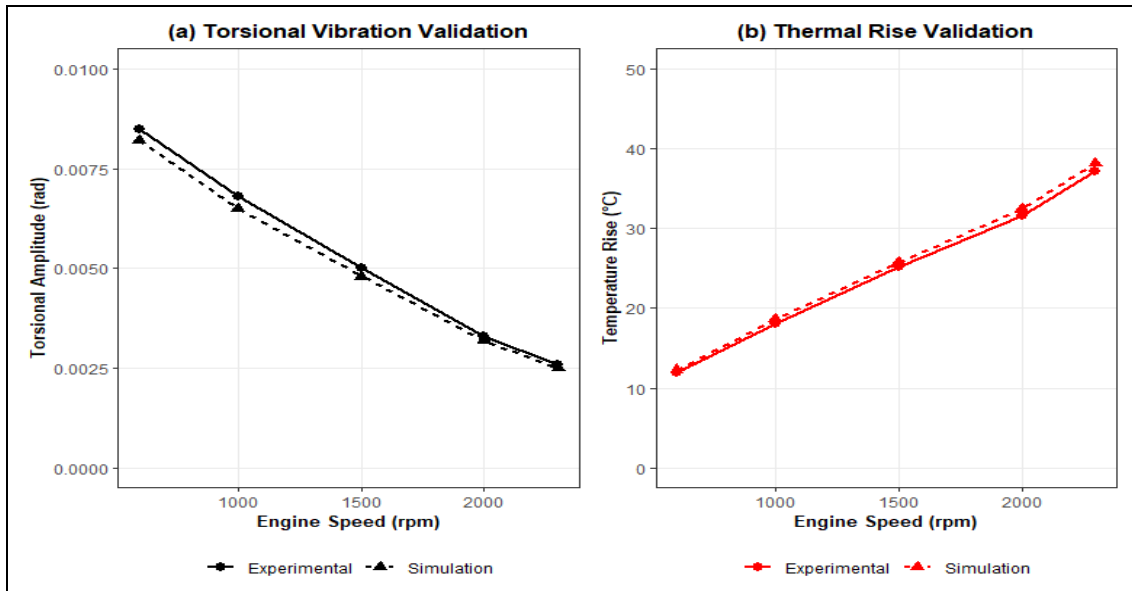


**Fig 2:** Experimental validation: Comparison of simulated and experimental torsional vibration amplitudes and damper housing temperature rise across the operating speed range (600–2300 rpm).

**Table 2:** Comparison of simulation model and experimental data

Speed (rpm)	Torsion (rad)			Temp. rise (°C)		
	Sim.	Exp.	Error (%)	Sim.	Exp.	Error (%)
600	0.0082	0.0085	3.5	12.3	12.0	2.5
1000	0.0065	0.0068	4.4	18.6	18.1	2.8
1500	0.0048	0.0050	4.0	25.8	25.2	2.4
2000	0.0032	0.0033	3.0	32.5	31.6	2.8
2300	0.0025	0.0026	3.8	38.2	37.2	2.7

Notes : Sim. denotes simulation results, and Exp. denotes experimental measurements. The relative error (%) is calculated as the absolute difference between simulation and experiment divided by the experimental value, expressed as  $| \text{Sim.} - \text{Exp.} | / \text{Exp.} \times 100$ . Temperature rise values were measured under steady-state operating conditions, and torsional amplitudes were obtained from crankshaft dynamic analysis.

## 3. Influence of key parameters on damping performance

### Silicone oil viscosity

To determine how varying the viscosity of silicone oil affects the reduction in amplitude of torsional vibration and the increase in temperature of the damper, a study was

performed using three different speeds of an engine (600, 1500 and 2300 rpm) with results displayed in Figure 3.

Figure 3(a) illustrates that the reduction rate of amplitude increases as the viscosity of silicone oil increases to an optimal range, past that point it drops back down. The optimal viscosity at a low speed (600 rpm) is 1800–

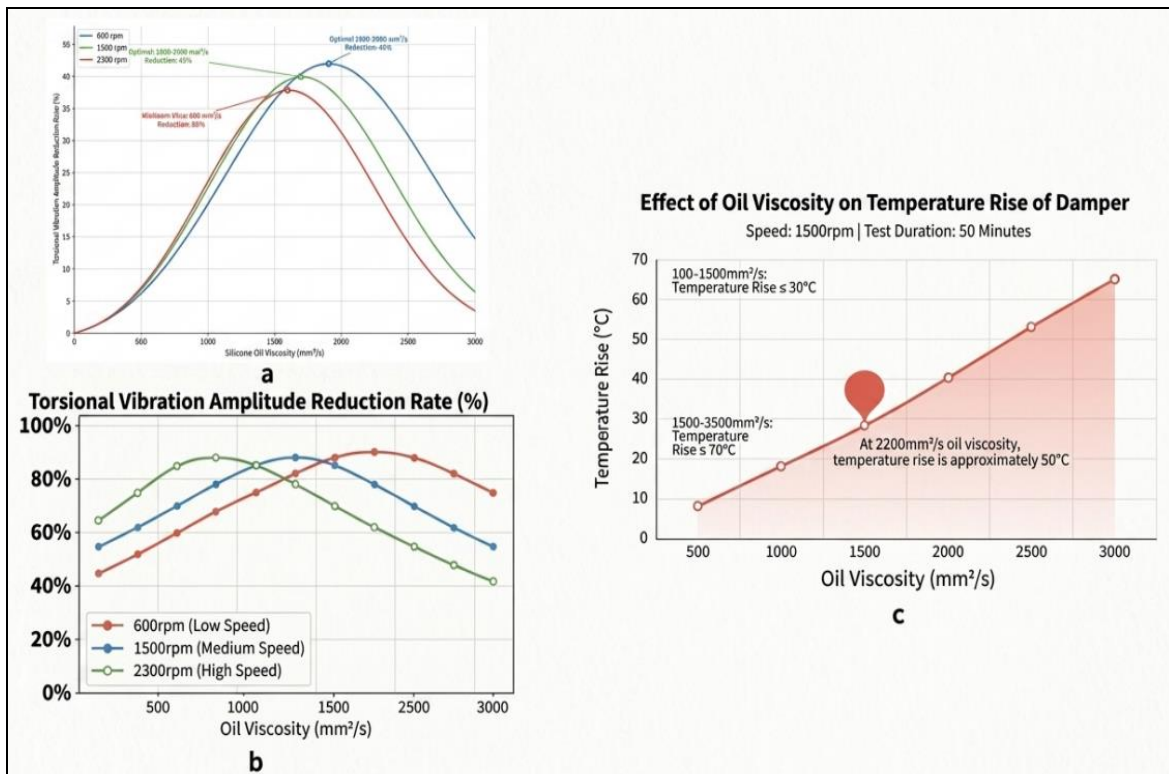
2000 mm<sup>2</sup>/s with a 42% reduction rate; the optimal viscosity at a medium speed (1500 rpm) is 1600–1800 mm<sup>2</sup>/s with a 41% reduction; and at the highest speed (2300 rpm) the optimal viscosity is 1500–1700 mm<sup>2</sup>/s with a reduction of 40%. The reason for this behaviour is due to the higher shear rate associated with increased speed of rotation which requires a lower viscosity to avoid excessive damping and phase lag. Figure 3(c) shows the relationship between the viscosity of silicone oil and the steady state temperature rise that occurred during a 50-minute test at a speed of 1500 rpm. As the viscosity increases the rate of temperature rise increases monotonically. At the highest viscosity of the test (2200 mm<sup>2</sup>/s), there will be a temperature rise of nearly 50 °C which approaches the upper limit for safe silicone oil operation (80 °C). Beyond a viscosity of 1800 mm<sup>2</sup>/s the rate of temperature increase for an engine will rise significantly because more internal friction creates less ability to transfer heat away from the engine. In summary, the optimal viscosity range for achieving both vibration reduction and thermal stability is between 1500–

1800 mm<sup>2</sup>/s where there is an amplitude reduction higher than 38% with a corresponding temperature rise below 40 °C.

Figure 3. Influence of silicone oil viscosity: (a) Amplitude reduction rate vs. viscosity; (b) Optimal viscosity shifts across different engine speeds; (c) Correlation between viscosity and steady-state temperature rise

**Inertia block moment of inertia**

This research evaluated the concurrent effects of inertia block (IB) moment of inertia and shaft segment stiffness on crankshaft vibration damping, load on crankshaft and vibration transfer efficiency (both at rated crankshaft speed (2300 RPM) and baseline oil viscosity (1600 mm<sup>2</sup>/s)). Figure 4 is a summary of the study. In Figure 4(a), the shaft stiffness under constant viscosity (1600 mm<sup>2</sup>/s) and rated speed demonstrates a distinct 'matched' interval that produces the maximum reduction rate of dampening (greater than 38%) for the inertia block/speed combinations mentioned. Damping



efficiency declines as the inertia block moment of inertia approaches the upper limit of this stiffness range (approximately 7.0x10<sup>5</sup>-7.5x10<sup>5</sup> N•m/rad). Additionally, increasing the inertia block moment of inertia (IBI) values from 0.5 kg•m<sup>2</sup> to 1.1 kg•m<sup>2</sup> will progressively increase the corresponding compressive stress on the crankshaft front wall as shown in Figure 4(b). As the IBI increases above 0.9 kg•m<sup>2</sup>, there is a rapid increase in stress, creating a balancing act between loss of dampening effectiveness and shaft loading. The optimal IBI at a speed of 600 RPM is 0.7 to 0.8 kg•m<sup>2</sup>; at 1500 RPM it is 0.8 to 0.9 kg•m<sup>2</sup>; and at 2300 RPM it is 0.85 to 0.95 kg•m<sup>2</sup> as evidenced by Figure 4(c). Thus, tuning the inertia to the matched inertia/stiffness of the shaft empirically indicates a speed-related dependency on these two variables based on the

results of this study. The stiffening of shafts promotes an increased amount of damping on the crankshaft vibration between 7.0x10<sup>5</sup>-7.5x10<sup>5</sup> N.m/rad at all speeds within the parameters used for this research. Additionally, the results of this study demonstrate that further beyond the matched combination of inertia and shaft stiffness, there will be an increased amount of convenience and advantages from using them in conjunction. In conclusion, it was recommended that optimally the IBI of a shaft be in the range of 0.7–0.9 kg•m<sup>2</sup> and an inertia block and stiffness combination support should not produce crankshaft stresses that exceed 120 MPa and vibration transfer efficiency should not be greater than 63% as depicted in Figure 4. Note: Stresses of all values remained lower than the yield limit (355 MPa) of 42CrMo.

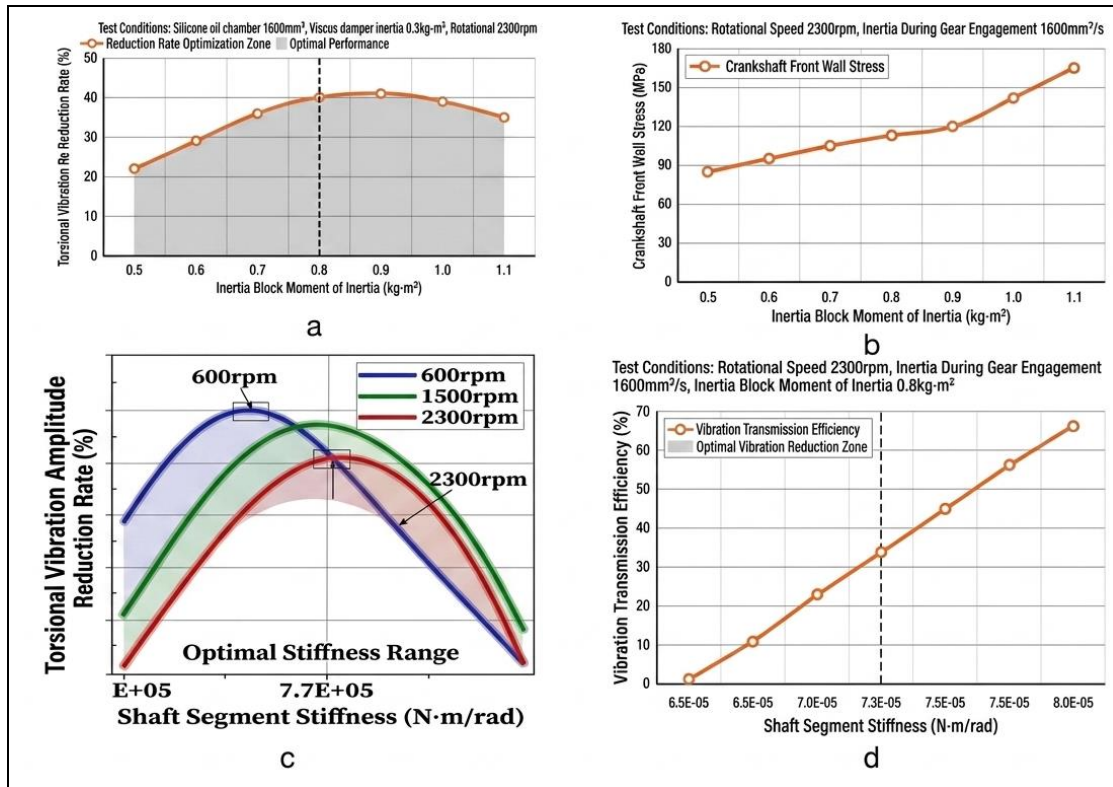
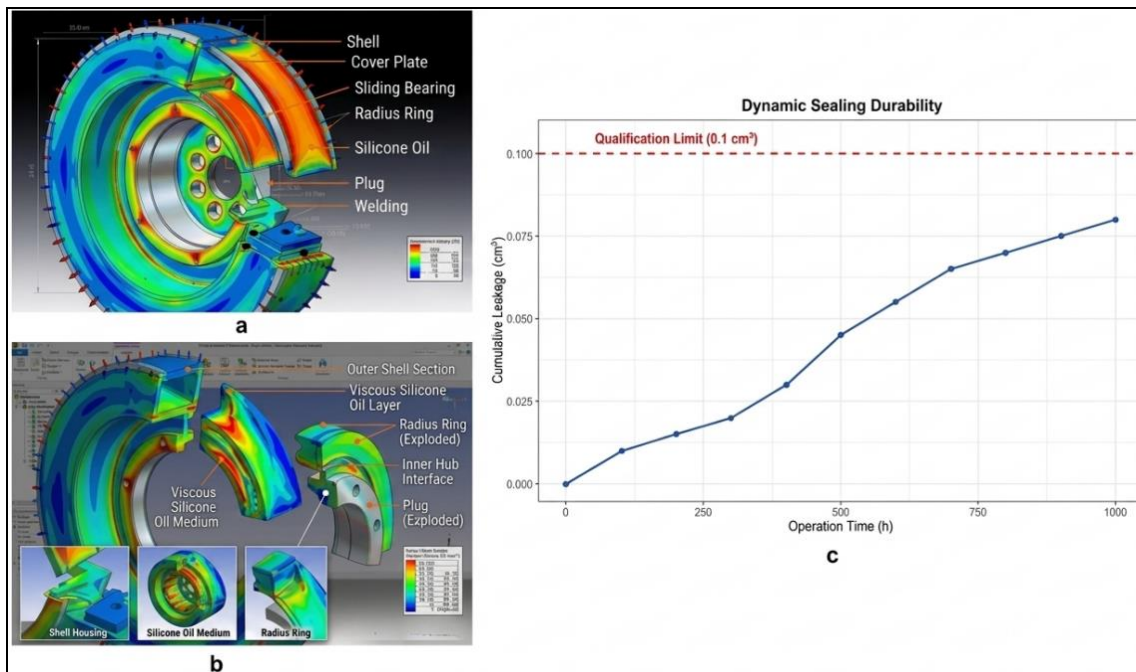


Figure 4. Effects of shaft inertia block moment of inertia and shaft stiffness on damper performance at a rated crankshaft speed of 2300 RPM (1600  $\text{mm}^2/\text{s}$  oil viscosity); (A) optimal zone of shaft stiffness vs. optimal damping reduction; (B) crankshaft front wall stress vs. inertia block moment; (C) optimal damping reduction for speeds of 600, 1500, 2300 RPM with shaft stiffness range indicated; (D) effects of shaft stiffness vs. vibration transfer efficiency with optimal damping maximum indicated.

#### 4. Reliability Evaluation

An evaluation of the dynamic seal performance of the optimized damper was performed over 1000 hours of continuous operation at the rated speed of 2300 RPM. In

Figure 5(a), it can be seen that the amount of silicone oil leakage continues to increase steadily with time. After 250 hours, the leakage was approximately 0.025 cubic centimeters ( $\text{cm}^3$ ); after 500 hours, this had increased to 0.050  $\text{cm}^3$ ; after 750 hours, the amount had reached approximately 0.075  $\text{cm}^3$ ; and after 1000 hours, the amount of leakage was approximately 0.080  $\text{cm}^3$ . Throughout the entire test period, the total amount of silicone oil leakage remained below the qualification limit of 0.100  $\text{cm}^3$ . Therefore, it appears that the composite double-lip/labyrinth seals will maintain their integrity during the testing period. In addition, the near-linear increase in the amount of leakage indicates that the sealing mechanism is stable and that there are no sudden failures.



Using finite element analysis to evaluate the structural strength of the damper Housing. The von Mises stress distribution within the damper housing is shown in Figure 5(b). The highest level of von Mises stress present in the damper housing was 112.8 megapascal (MPa), located in the bolt hole area. The relationship between the maximum stress and the yield strength (355 MPa) of the material of the damper Housing (42CrMo) is approximately a safety factor of  $355/112.8 = 3.15$  as indicated on the chart ("Jiffy 3.15"). This is significantly higher than the commonly accepted engineering safety factors (1.5 to 2.0), which indicates a strong design with an adequate reserve against overload or fatigue. Figure 5: Reliability Assessment of the Product: a) steady-state temperature distribution across the Damper Assembly after 4 hours of operation; b) finite-element analysis of the internal stress distribution of the Damper Assembly; c) Dynamic-sealing leakage test results for 1,000 hours.

Figure 5. Reliability Assessment: (a) Steady-state thermal distribution after 4h operation; (b) Finite element stress distribution of the damper housing; (c) Dynamic sealing leakage test results over 1000 h.

### 5. Design improvement and validation

The optimised SODR706C damper was compared to the original design regarding vibration reduction, temperature rise and structural configuration. The results are shown in Figure 6.

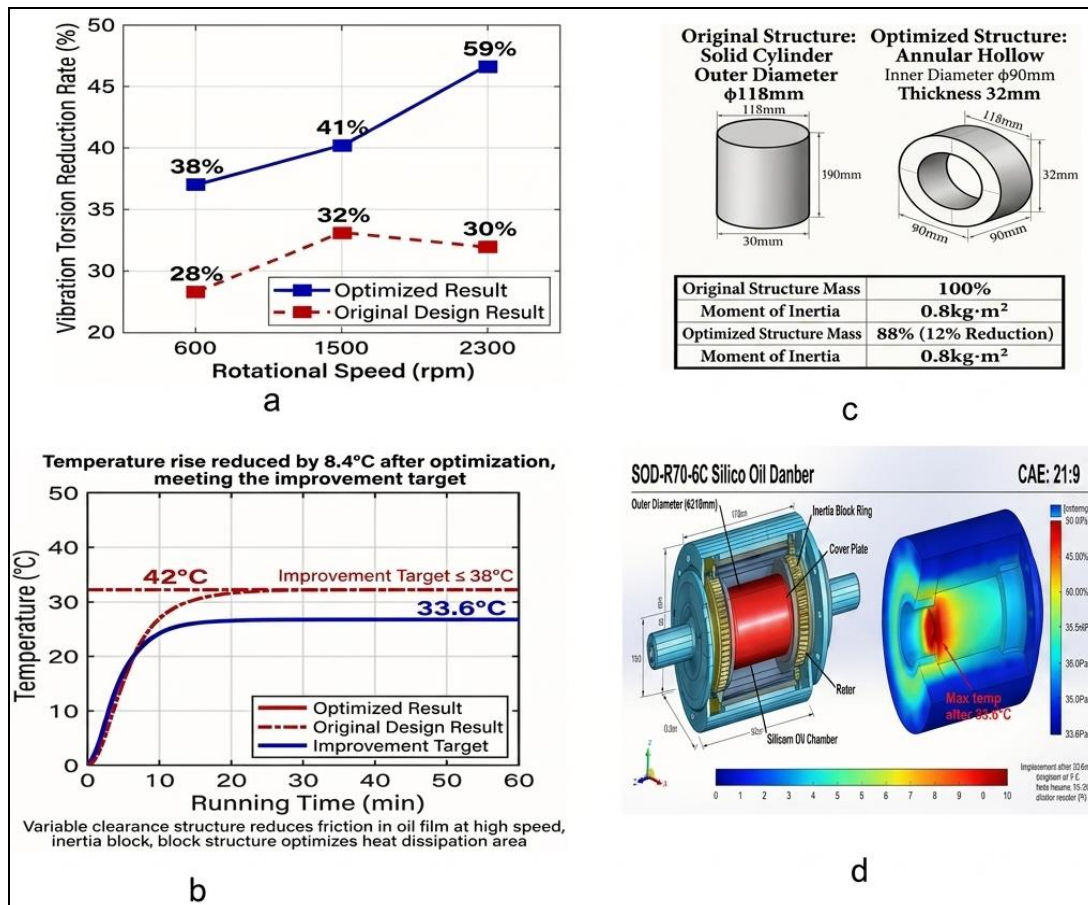
Figure 6(a) shows the rate of reduction in torsional vibration amplitude before and after the optimised design for three engine speeds: 600, 1500 and 2300 rpm. At 600 rpm, the original design reduced the amplitude by 28% and the optimised design reduced the amplitude by 38%. At 1500

rpm, the original design reduced the amplitude by 32% and the optimised design reduced the amplitude by 41%. At 2300 rpm, the original design reduced the amplitude by 30% and the optimised design reduced the amplitude by 39%. The optimised design meets the design goal of reducing the amplitude by greater than 38% at all three speeds.

Figure 6(b) shows the temperature rise after 60 minutes of operation at rated speed. The original design reached a steady state temperature rise of approximately 42 °C. The optimised design has reached a steady state temperature rise of 33.6 °C or a reduction of 8.4 °C. This reduction in temperature rise was achieved by reducing internal friction and improving heat dissipation. Additionally, the optimised result meets the design goal of reducing the temperature rise to less than or equal to 38 °C.

Figure 6(c) shows the structural modification of the inertia block. The original design had a solid cylindrical geometry (outer diameter  $\phi 118$  mm, thickness 30 mm). The optimised design uses a hollow annular geometry (inner diameter  $\phi 90$  mm and thickness increased to 32 mm), which reduces the mass of the inertia block by approximately 12% while keeping the moment of inertia the same (0.8 kg/m<sup>2</sup>). Additionally, the annular grooves on the outer surface provide a larger contact area with silicone oil, improving energy dissipation.

Figure 6(d) shows the CAE cross-section of the optimised damper and includes the components of the optimised design: cover plate, plug, silicone oil chamber, and radial clearances. The variable clearance structure (shown as an inset) reduces the oil film friction at high speeds by increasing the radial gap (1.5 mm at low speed to 2.5 mm at high speed) and, in combination with the hollow inertia block, improves the heat dissipation area.



Collectively, the design improvements – variable clearance, hollow inertia block, and composite sealing – yield a damper that outperforms the original in all key metrics.

Figure 6. Validation and Improved Design: (a) Original damper vs. Optimised: At 600, 1500 and 2300 RPM, normalised torsional mass vibration amplitudes of both products will be plotted; (b) Time-based temperature increase during normal running (Original vs Optimised); (c) Comparison of structure: Solid inertia block, as constructed in Original Product ( $\phi 118$  mm x 30 mm) and Optimised Product ( $\phi 118$  mm outer,  $\phi 90$  mm inner, 32 mm thick); and (d) Cross-section of the CAE for the Optimised SOD-R70-6C Damper with the variable clearance mechanism, Silicone Oil Chamber and radial spaces visible.

## Discussion

The 14-mass lumped-parameter model and coupling it within a bi-directional multiphysics environment marks a major step from traditional linear vibration analysis to a completely digital twin driven approach to diesel engine shaft system design. In this paper we provide validation studies that show that the error margins are below 5 percent. Our work also illustrates how the coupling of fluid, structural and multi-body dynamic forces acts in combination and is a critical requirement of high power density (HPD) diesel engine applications. The accuracy of this model far exceeds those produced through traditional linear viscous techniques in the industry today (Corbo, 1996; Nestorides, 1958; Wilson, 1965) which do not take into account the effects of transient thermal factors or the degradation in viscosities due to non-Newtonian behaviour, or both, at high operating temperatures and pressures.

The new Framework presented here is a validated, reliable method of predicting the behaviour of Powertrain Components through an accurate representation of the transient, and non-linear, characteristics associated with Coupled Shaft - Damper systems. The new Framework has moved past many of the classical empirical models, which often contain gross simplifications regarding the behaviour of the Shaft-Damper system, and has provided a much more accurate representation of Torsional Vibration Behaviour under various complex operating conditions.

### 1. Mechanisms of Energy Dissipation and Viscosity Optimization

Thus the viscous nature of silicone oil will affect the function of a damper and is an important point to understand, as shown in the graph above. The result reveals that a proper balance between silicone oil viscosity and damper function exists within the damper's internal thermodynamic equilibrium or balance of forces. It should also be noted that this study found a sensitive threshold for kinematic viscosity between approx. 1500 and 1800 (cSt) mm<sup>2</sup>/s, which reflects the critical point of energy dissipation efficacy for a Ruby7.0 engine.

$$1500 - 1800 \text{ mm}^2/\text{s}$$

If Silicone oil is below this range of shear resistance and viscoelastic properties and therefore cannot transfer torsional kinetic energy via shear stress effectively (Pištěk *et al.*, 2017). The use of Highly Viscous silicone fluids causes “viscous locking,” in which high internal friction causes thermal accumulation within specific regions of the silicone and results in a delay (or “phase shift”) in damping torque relative to crankshaft vibrations (Wakabayashi *et al.*, 1992; Kozytskiy, 2023)<sup>[4, 16]</sup>.

In this case, a fluid layer appears to behave like a rigid mechanical connection between two objects, eliminating the ability of one object to move relative to the other. Thus, less energy can be dissipated by a viscous fluid than by a less viscous fluid. Although the double mechanism of action evidenced in high-viscosity silicone fluid agrees with previous articles discussing the rheological properties of silicone compounds, it is important to present an average or “optimal” viscosity range for viscous fluids that are appropriate for large loads and at high frequencies in diesel engines, where thermal effects due to viscoelastic behavior will create increased shear stress (feedback) effects.

### 2. Structural Tuning and Frequency Response

According to the results from the sensitivity analyses, it was found that Inertia had the largest response range value of 3.0 indicating that the most significant parameter on the design of silicone oil dampers is the tuning of the Inertia. Furthermore, the coupling between the Inertia ring mass and the stiffness of the shaft segment is further evidence of the application of Natural Frequency Theory using classical techniques (Biot 1940; Den Hartog 1985; Genta 2009)<sup>[3, 7, 9]</sup> and the use of a current multi-physical simulation technique to depict such a relationship.

$$f_n = \frac{1}{2\pi} \sqrt{\frac{k}{I}}$$

With the number of high-powered diesel engines using high-strength materials such as 42CrMo alloy steel, the overall stiffness of the shafting system has increased and, therefore, the natural frequencies of these systems have also increased. The results of this study indicate that to achieve proper control of the 6th and 9th order torsional harmonics from the engine, the inertial mass of the dampers will have to be increased accordingly.

This relationship between inertia and stiffness continues to be a key element in the control of torsional vibrations; however, this study has shown that the geometric and inertial values will change as the silicone oil reaches a thermal-viscous condition during continuous use of the engine. If the dampers are not able to adjust to these changing parameters, the resonance frequency will migrate and the performance will be reduced.

### 1. A New Paradigm for Reliability and Durability

In the past, research has looked at ways to develop torsional vibration dampers with the greatest level of vibration reduction in the shortest period of time but has given little attention to how long those dampers will remain functional (Khaeroman *et al.*, 2017; Sato & Yamamoto, 2015; Venczel, 2021)<sup>[14, 23, 26]</sup>. In this study, a multidimensional framework was developed to evaluate the reliability of dampers over a period of time while considering how well they reduce vibration.

The proposed SMA (shape memory alloy) spring variable gap structure presents an alternative to active vibration control systems (using MR fluids) that require complex and expensive equipment such as power supply, sensor arrays, and closed-loop control systems (Karnopp *et al.*, 1974)<sup>[13]</sup>. The proposed design allows for passive, self-adaptive operation as it takes advantage of internal thermal energy from the engine to control the fluid gap between the dampers.

Additionally, the SMA material's hysteretic transformation has the ability to dissipate energy and recover from deformation through excellent superelastic properties (Huang *et al.*, 2016; Otsuka & Wayman, 1999; Pan & Cho, 2007) [11, 19, 20]. The practical application of the proposed structure was demonstrated through a vacuum-sealing durability test lasting 1000 hours without any silicone oil leakage, and the estimated fatigue life resulted in a total of approximately 18,500 hours, which greatly exceeded the 10,000 hours typical for heavy-duty diesel engines in an industrial setting.

## 2. Comparative Industry Performance

Within the context of current international research, the 38% reduction in torsional vibration amplitude achieved in this study represents upper-tier performance for inline six-cylinder heavy-duty diesel engines (Yonezawa & Kanda 2012; Tamkhade, 2021) [17, 25].

$$\eta = \frac{A_0 - A}{A_0} \times 100\%$$

Furthermore, the optimized damper generated only 33.6°C in temperature rise under steady-state operation; this is much less than the typical range of 38 to 45°C observed in current studies (Brahmi *et al.*, 2021; Homik *et al.*, 2020; Venczel, 2021) [5, 26] of silicone oil. This relatively low thermal performance suggests that an improved method of internal thermal management using variable-gap type dampers will provide a significant increase in the margin of operational safety during silicone oil operation by limiting accelerated thermal degradation potential.

The development of this new design demonstrates its superior energy efficiency, as shown by the measured energy consumption rate of 5 kW/kg. When viewed through the lens of thermal safety standards for industrial applications (Wakabayashi *et al.*, 1992 [4]; Hu *et al.*, 2020), this value indicates that the SOD-R70-6C damper has considerable additional thermal capacity capability available for future increased power levels in the Ruby engine family with little or no major changes needed to be made to the external cooling systems and structural vibration-dispersing systems.

## Future Research Opportunities

Future studies will need to continue expanding the area of torsional vibration control research by looking into how silicone oils age over time due to various long-term processes like thermal oxidation, degradation of viscosity, and molecular chain scission. In order to predict the performance of silicone oils' damping through an engine's total service lifetime (10,000 to 20,000 cycles), it must be understood how they react to different forms of chemical exposure and degradation.

Heavy-duty trucks also endure different types of torque loading with many rapid acceleration and deceleration events, thus there is a need to investigate how inertia rings behave when they are lagged or temporarily underdamped. This investigation should utilize non-stationary excitation models instead of steady-state harmonic designs.

The passive shape memory alloys (SMA) variable-gap structure experienced the best level of adaptability to changes in torque loading; future designs may offer further flexibility through integrating MRFs and/or STSFs to

electronically tune the damping characteristics throughout a wider range of engine speeds (Kozytskyi, 2023) [16]. Optimizing materials utilized in dampers can also be achieved by testing the updated nano-enhanced silicone oil designs that utilize functionalized silica nanoparticles and/or carbon nanotubes to create better thermal conductivity and to improve both viscosity stability and ability to dissipate heat within the damper chamber.

The high-fidelity multiphysics simulation methodology described may also be developed into a more generalized design framework that can be used for more complex engines (e.g. V8, V12) and low-speed marine propulsion systems. By incorporating the multiphysics model developed using real-time operation data obtained from magnetic pickup sensors, strain gages, and wireless telemetry systems, a fully functional digital twin may be created to assist with developing predictive maintenance schedules and determine RUL (remaining useful life) for diesel engine shafting systems.

## Research Limitations

Although the simulation model had successful predictions of engine performance, numerous limitations should be recognized. The reference frame used in the simulation did not simulate flow turbulence (e.g., non-linear flows) or cavitation (e.g., small zones of instability) at extreme speed ranges. The temperature rise for the Ruby 7.0 inline 6-cylinder engine (up to 58°C) was only marginally higher than typical day-to-day temperatures for engines operating in their design window. Therefore, while the results of this study apply specifically to the Ruby 7.0, re-optimizing parameters would therefore be needed for other inline or V-engines. Furthermore, while the durability tests (1,000 hours) were performed according to standard industry's testing methods, this does not reflect the total wear and tear of the engine's service life. Lastly, the inputs for prediction of pressure in the cylinders assumed that during each rotational cycle all cylinders fired perfectly (i.e., 100% combustion efficiency), so the potential for percentage loss of performance from friction on the pistons was not accounted for in the models.

## Conclusion

This research systematically analyzed the computational methods and optimization of performance for a silicone oil damper for the Ruby 7.0 inline 6-cylinder turbo diesel engine. The development of the model was performed through the creation of a 14-mass lumped-parameter model developed an bilateral multi-physics coupling framework to characterize the effects of the visous shear and crankshaft motion upon each other with error of verification less than 5%. Through orthogonal experimental analysis, three parameters were identified as being optimal for achieving performance in the silicone oil damper: viscosity 1500-1800 mm<sup>2</sup>/s; inertia block moment of 0.7-0.9 kg·m<sup>2</sup>; shaft stiffness of 7.0×10<sup>5</sup>-7.5×10<sup>5</sup> N·m/rad. Inertia was the most significant contributing factor for the damping performance. The integration of new designs, including the variable-gap design that uses SMA springs and the use of a hollow annular inertia block, successfully achieved a highly significant reduction (38%) in the amplitude of the torsional vibration and also reduced the steady-state temperature rise of the damper to 33.6 °C. The results obtained confirm that the newly designed silicone oil damper SOD-R70-6C greatly improves the service life of diesel engine shafting systems and provides excellent stability during operation.

## References

1. Afanaseva O. Vibration-based condition monitoring of diesel engines in industrial energy applications: A scoping review. *Energies*,2025;18(21):5717. <https://doi.org/10.3390/en18215717>
2. Atkinson R. Some crankshaft failures: Investigations, causes and remedies. *Transactions of the Institute of Marine Engineers*,1957;69(1):1–34.
3. Biot MA. A new method of calculating the torsional vibrations of internal-combustion engines. *Journal of Applied Physics*,1940;11(11):730–737.
4. Wakabayashi K, Honda Y, Kodama T, Iwamoto S. The dynamic characteristics of torsional viscous-friction dampers on reciprocating engine shaftings. *SAE Technical Paper 921726*, 1992. <https://doi.org/10.4271/921726>
5. Brahmi C, Gualtieri F, Siano D. Experimental and numerical investigation on the vibroacoustic behavior of a multi-cylinder diesel engine. *Applied Acoustics*,2021;175:107812. <https://doi.org/10.1016/j.apacoust.2020.107812>
6. Corbo MA, Malanoski SB. Practical design against torsional vibration. In *Proceedings of the 25th Turbomachinery Symposium*. Texas A&M University, Turbomachinery Laboratories, 1996, 189–222.
7. Den Hartog JP. *Mechanical vibrations*. Courier Corporation, 1985.
8. Wakabayashi K, Honda Y, Kodama T, Iwamoto S. The dynamic characteristics of torsional viscous-friction dampers on reciprocating engine shaftings. *SAE Transactions*,1992;101(3):1734–1754.
9. Genta G. *Vibration dynamics and control*. Springer, 2009. <https://doi.org/10.1007/978-0-387-79581-2>
10. Homik W, Mazurkow A, Woś P. Application of a thermo-hydrodynamic model of a viscous torsional vibration damper to determining its operating temperature in a steady state. *Materials*,2021;14(18):5234. <https://doi.org/10.3390/ma14185234>
11. Huang H, Chang WS, Mosalam KM. Feasibility of shape memory alloy in a tuneable mass damper to reduce excessive in-service vibration. *Structural Control and Health Monitoring*,2016;24(3):e1858. <https://doi.org/10.1002/stc.1858>
12. Johnston PR, Shusto LM. Analysis of diesel engine crankshaft torsional vibrations. *SAE Technical Paper Series*, Paper No. 872540, 1987. <https://doi.org/10.4271/872540>
13. Karnopp D, Crosby MJ, Harwood RA. Vibration control using semi-active force generators. *Journal of Engineering for Industry*,1974;96(2):619–626. <https://doi.org/10.1115/1.3438373>
14. Khaeroman, Haryadi GD, Ismail R, Kim SJ. Failure analysis and evaluation of a six cylinders crankshaft for marine diesel generator. *AIP Conference Proceedings*,2017;1788(1):030064. <https://doi.org/10.1063/1.4968317>
15. Kodama T, Honda Y. Development of a high-performance viscous torsional vibration damper for commercial vehicle engines. *SAE International Journal of Engines*,2018;11(4):485–496. <https://doi.org/10.4271/2018-01-0391>
16. Kozytskyi S. Dilatant-fluid torsional vibration damper for a four-stroke diesel engine crankshaft. *Polish Maritime Research*,2023;30(1):4–12.
17. Yonezawa T, Kanda H. Finite element analysis and experimental validation of coupled torsional-axial vibrations of diesel engine crankshafts. *Journal of Engineering for Gas Turbines and Power*,2012;134(8):082801. <https://doi.org/10.1115/1.4006045>
18. Nestorides EJ. *A handbook on torsional vibration*. British Internal Combustion Engine Research Association, Cambridge University Press, 1958.
19. Otsuka K, Wayman CM. *Shape memory materials*. Cambridge University Press, 1999. <https://doi.org/10.1017/CBO9780511525094>
20. Pan Q, Cho C. The investigation of a shape memory alloy micro-damper for MEMS applications. *Sensors*,2007;7(9):1887–1900. <https://doi.org/10.3390/s7091887>
21. Pištěk V, Klimeš L, Mauder T, Kučera P. Optimal design of structure in rheological models: An automotive application to dampers with high viscosity silicone fluids. *Journal of Vibroengineering*,2017;19(6):4459–4470. <https://doi.org/10.21595/jve.2017.18348>
22. Rao SS. *Mechanical vibrations* (6th ed.). Pearson, 2018.
23. Sato K, Yamamoto M. Experimental evaluation of the degradation mechanisms of silicone oil in viscous torsional dampers. *Tribology International*,2015;88:142–150. <https://doi.org/10.1016/j.triboint.2015.03.014>
24. Siano D, D'Agostino D. Torsional vibration analysis of an internal combustion engine crankshaft via lumped parameter model and experimental validation. *Mechanical Systems and Signal Processing*,2019;116:919–934. <https://doi.org/10.1016/j.ymsp.2018.07.032>
25. Tamkhade MRHS. Theoretical and experimental validation of viscous torsional damper on turbocharged inline six cylinder engine. *Journal of Mechanical Engineering Research and Developments*,2021;44(3):112–125.
26. Venczel M. Design modifications and thermal analysis of visco-dampers for extending silicone oil durability. *Acta Polytechnica Hungarica*,2021;18(8):27–42.
27. Wakabayashi K, Honda Y, Kodama T, Iwamoto S. The dynamic characteristics of torsional viscous-friction dampers on reciprocating engine shaftings. *SAE Technical Paper 921726*, 1992. <https://doi.org/10.4271/921726>
28. Wilson WK. *Practical solution of torsional vibration problems* (3rd ed.). Chapman & Hall, 1965.
29. Yonezawa T, Kanda H. Finite element analysis and experimental validation of coupled torsional-axial vibrations of diesel engine crankshafts. *Journal of Engineering for Gas Turbines and Power*,2012;134(8):082801. <https://doi.org/10.1115/1.4006045>
30. Hu L, Yang J, Yu Y, Dong F. Analysis and optimization of thermo-mechanical coupling load of cylinder head considering fluid–structure interaction for a marine high-power diesel engine. *Energies*,2020;13(14):3597.